European Review for Medical and Pharmacological Sciences 2022; 26: 1283-1292

Experimental study on thioredoxin redox inhibitor 1-methylpropyl 2-imidazolyl disulfide promoting apoptosis of multiple myeloma cells *in vitro* and *in vivo*

Q.-D. LIN[1,2,3,4], L.-N. LIU[1,2,3,4], X.-Y. LIU[1,2], Y. YAN[1,2], B.-J. FANG[1,2,3,4], Y.-L. ZHANG[1,2,3,4], J. ZHOU[1,2,3,4], Y.-F. LI[1,2,3,4], W.-L. ZUO[1,2,3,4], Y.-P. SONG[1,2,3,4]

[1]Affiliated Cancer Hospital of Zhengzhou University, Zhengzhou City, Henan Province, China
[2]Henan Cancer Hospital, Zhengzhou City, Henan Province, China
[3]Henan Key Lab of Experimental Hematology, Zhengzhou City, Henan Province, China
[4]Henan Institute of Hematology, Zhengzhou City, Henan Province, China

Abstract. – OBJECTIVE: To explore the *in vitro* and *in vivo* experimental study of thioredoxin-1(Trx1) inhibitor 1-methylpropyl 2-imidazolyl disulfide (PX-12) promoting multiple myeloma H929 cell apoptosis, investigate the relationship between the inhibitory effect of PX-12 on H929 cells and reactive oxygen species (ROS).

MATERIALS AND METHODS: Inhibition of PX-12 on H929 cells in relation to reactive oxygen species (ROS), cell cycle, and apoptosis were assessed by flow cytometry. ELISA kit, IVIS Imaging, Hematoxylin and eosin (H&E) staining and immunohistochemical staining assessment were applied to assess the anti-myeloma effect in the SCID mice model established by H929EL cells.

RESULTS: PX-12 inhibited proliferation of H929 cells performed time and dose dependent style. Furthermore, it significantly induced a G2/M phase arrest of the cell cycle in H929 cells. It also increased intracellular ROS and caspase-3 activity in H929 cells indicating that cells have undergone apoptosis. There was an almost 3-5-fold decrease in tumor viability measured by the Living-Imaging system after 21 and 28 days after PX-12 injection compared with the control group. Importantly, PX-12 caused significant decrease in expression of Kappa chain *in vivo* assessed by immunohistochemical staining.

CONCLUSIONS: The results suggest that PX-12 may be a potential strategy for the treatment of MM, and the inhibition of TRX-1 in the treatment of myeloma deserves further research.

Key Words:
Thioredoxin-1 (Trx1), PX-12, Reactive oxygen species (ROS), Multiple myeloma cells.

Introduction

Multiple myeloma (MM) is a tumor characterized by abnormal proliferation of monoclonal plasma cells in bone marrow which can secrete large amounts of abnormal monoclonal immunoglobulin, and thus causing a series of clinical symptoms. The incidence of MM accounts for 2% of all tumors and is the second highest incidence of hematological malignancies[1]. The application of proteasome inhibitor (PIs), immunomodulator (IMiDs), monoclonal antibody (CD38/SLAMF7) and chimeric antigen receptor cell therapy (CAR-T) significantly improved the efficacy of multiple myeloma patients[2-6]. Although great progress has been made in the treatment of myeloma, it is still an incurable disease, and the 5-year median survival rate has not improved significantly[7]. Many patients develop resistance, therefore, there is an urgent need for new therapeutic targets to overcome drug resistance.

Thioredoxin system is an important antioxidant system to maintain the intracellular redox status, which is composed of thioredoxin (Trx), thioredoxin Reductase (Trx-R) and NAPDH[8]. Trx system consists of thioredoxin 1 (Trx-1), a cellular redox protein, thioredoxin reductase 1 (TrxR1) enzyme, and NADPH. The expression of TRX-1 is increased in many tumors, which is related to tumor cell proliferation, survival and chemotherapy resistance[9-11]; moreover, it is also related to cell survival, tumor metastasis and angiogenesis[12,13], and its inhibition could result in cancer cell apoptosis[14]. It was already shown that the expression of Trx-1 was inhibited by the Si-RNA technology or that Trx-1 inhibitors can promote tumor cell apoptosis and enhance the sensitivity of tumor cells to chemotherapy drugs[15]. PX-12,1- methylpropyl-2-imidazolyl disulfide is a kind of TRX-1 inhibitor, which irreversibly binds to TRX-1 and inactivates TRX-1 redox, showing antitumor ac-

Corresponding Author: Yongping Song, MD; e-mail: songyongping001@126.com

tivity both *in vitro* and *in vivo*[16,17]. It was reported that the level of trx-1 decreased more significantly in patients treated with px-12 for 3 hours than that in patients treated for 1 hour, Px-12 also reduced the level of plasma vascular endothelial growth factor (VEGF) in tumor patients[18]. As for the hematological malignancies, Shao et al[19] investigated the expression of thioredoxin in T-cell acute lymphoblastic leukemia (T-ALL), the results showed that thioredoxin was expressed in different degrees in T-ALL, and PX-12 could inhibit leukemia colony formation in primary T-ALL. Kari et al[20] have demonstrated Trx-1 level was highly expressed in the Diffuse Large B cell Lymphomas (DLBCL) patients, which indicated disease progression, chemotherapy resistance and low survival rates, they found that cell proliferation and colony formation of DLBCL cells could be inhibited by SiRNA and Trx-1 inhibitor PX-12, as well as the sensitivity to doxorubicin could be enhanced, suggested its anti-tumor effect in relapsed/refractory DLBCL patients. Tan et al[21] also found that PX-12 can promote the apoptosis of acute myeloid leukemia (AML) cells and enhance the sensitivity of AML cells to arsenic trioxide, suggesting that PX-12 has therapeutic potential for AML. Raninga et al[22] proved Trx-1 inhibitor PX-12 can induce apoptosis in resistant multiple myeloma cells, however, the *in vivo* inhibitory effect of Trx-1 inhibitors on multiple myeloma cells has not been explored. This study explored the role of PX-12 in multiple myeloma SCID mouse model on the basis of *in vitro* experiments, in order to lay a foundation for further clinical research.In this study, the effect of PX-12 on the activity of MM cells was observed, the cell cycle and apoptosis rate were detected by flow cytometry, and the level of intracellular reactive oxygen species (Ros) was detected by H2D-CFDA probe. Beyond this, the SCID-RAB mice model established by MM cells was applied for the *in vivo* study, tumor proliferation was monitored by the Living-Imaging, serum Trx-1 level was detected before and after administration of PX-12, to explore the efficacy of PX-12 in the treatment of myeloma mice model by HE staining and Kappa antibody staining.

Materials and Methods

MM Cell Line and Growth

H929 cells were grown *in vitro* in Roswell Park Memorial Institute-1640 (RPMI-1640) medium (Sigma-Aldrich, St. Louis, MO, USA), supplemented with 10% fetal bovine serum (FBS; Sigma-Aldrich) and 1% penicillin-streptomycin (Gibco BRL, Grand Island, NY, USA), and stored in a humidified incubator containing 5% CO_2 at 37°C. To track the metastasis of H929 cells *in vivo*, we infected H929 cells with lentivirus containing Luciferase/green fluorescent protein and quantified it.

Reagents

PX-12 was purchased from Sigma-Aldrich and dissolved in dimethyl sulfoxide (DMSO; Sigma-Aldrich, St. Louis, MO, USA) at 10 mM as raw solution. NAC and BSO were obtained from Sigma-Aldrich. NAC was dissolved in 20 mM HEPES buffer (pH 7.0) and BSO was dissolved in water. H929 cells were pretreated with 2 mM NAC or 10 μM BSO for 1 h prior to treatment with PX-12. DMSO (0.2%) was used as a control vehicle.

Growth Inhibition Assay

The effects of PX-12 on cell growth were detected by measuring 3-(4,5-dimethylthiazol-2-yl) -2,5-diphenyltetrazolium bromide (MTT; Sigma-Aldrich) absorbance in living cells. In brief, 1×10^4 cells/well were plated in 96-well plates (R&D Systems). After the action of a specified dose of PX12 for a specified time, MTT solution [20 μl: 2 mg/ml phosphate-buffered saline (PBS)] was added to each well. The plate was incubated at 37°C for 3 hours, the liquid was transferred, and 200 μl dimethyl sulfoxide (DMSO) was added to each hole to dissolve formaldehyde crystal. The optical density was measured at 570 nm using a microplate reader.

Cell Cycle Analysis

Cell cycle and sub-G1 cell analysis were detected by propidium iodide (PI, BD Biosciences, Franklin Lakes, NJ, USA) staining. In brief, 1×10^6 cells were incubated in a 60-mm culture dish (R&D Systems, Minneapolis, MN, USA) and treated with the designated doses of PX-12 for 72 h, then washed by PBS and fixed in 70% (v/v) ethanol. After removing the residual ethanol, add PI (10 μl of 50 μg/ml), ribonuclease A (50 μl, 1 mg/ml, Sigma Aldrich, St. Louis, MO, USA) and 0.1% bovine serum albumin (BSA; 200 μl) were added to the cells. After incubating 30 min without light, the cell cycle was analyzed by BD Biosciences flow cytometry.

Cell Death Detect

Cell death was detected by Annexin V fluorescein isothiocyanate (FITC)/PI staining. Apopto-

sis was determined by Annexin V FITC staining (Ex/Em=488/519 nm; Invitrogen Life Technologies, Camarillo, CA, USA). In brief, 1×10^6 cells were incubated with a specified dose of PX12 in a 60 mm petri dish for 72 hours, with or without 2 mM NAC or 10 μM BSO. The cells were washed twice with cold PBS, then suspended in 500 μl binding buffer with a concentration of 1×10^6cells/ml, and then added Annexin V FITC (5 μl) and PI (5 μl) to analyze the cells.

In order to observe the effect of GSH precursor NAC (N-acetyl cysteine) and inhibitor BSO (L-buthionine sulfoximine) on apoptosis induced by PX-12, cells were pre-incubated with 2 mM NAC or 10 μM BSO for 1 h, and then treated with 10 μM PX-12 for 72 h. Apoptosis was detected by FACStar flow cytometry.

Detection of Intracellular ROS Levels

Intracellular ROS levels were detected by oxidation-sensitive fluorescent probe, 2',7'-dichlorodihydrofluorescein diacetate (H2DCFDA; Ex/Em=495/529 nm; Invitrogen Life Technologies, Carlsbad, CA, USA). In brief, 1×10^6 cells were incubated in 60-mm culture dish with a specified dose of PX-12 for 72 h with or without 2 mM NAC or 10 μM BSO.

The cells were washed with PBS buffer and incubated with 20 μM H2DCFDA at 37°C for 30 min. The fluorescence level of H2DCFDA was detected by flow cytometry. The level of ROS was expressed by the average fluorescence intensity calculated by CellQuest software (BD).

Mice model establishment and IVIS Imaging measurement

SCID Mice Were Obtained from Harlan Laboratories (IN, USA).The mouse model was established by implanting bilateral femurs of New Zealand white rabbits into the back of mice. Four weeks after the implantation, 5×10^6 H929 cells labeled with Luciferase green fluorescent protein were directly injected into the implanted rabbit bone on the right back of the model mice (Rabbit bone was implanted subcutaneously on the back of mice). MM progression in mice was monitored by measuring *in vivo* biological imaging (IVIS Imaging system; Perkin Elmer, Waltham, MA, USA)[23]. Mice model were administered PX-12 (dissolved in DMSO) or vehicle (mice/group), 25 mg/kg intravenously for 6 weeks[18]. ELISA kit assays were used to measure serum Trx-1 level at the indicated time points, tumor burden was monitored by the IVIS-Imaging every 7 days.

Evaluation of Hematoxylin Eosin (H&E) Staining and Immunohistochemical Staining

To observe the *in vivo* effect of PX-12 on H929/EL cells, the mice were anaesthetized with ketamine and serazine at the end of the experiment, and the mice were sacrificed by cervical dislocation. Xenografts were isolated from the sacrificed mice, tissue specimens were fixed in formalin containing 10% phosphate buffer for 24 hours, decalcified with EDTA (10% wt/vol, pH 7.0) and embedded in paraffin. The slices (5 μm) were degreased with xylene, rehydrated with ethanol, rinsed with normal saline and antigen retrieval with microwave. According to the manufacturer's instructions, the tissue sections were stained with HE staining kit (catalog number, C0105, Beyotime Institute of Biotechnology), or incubated with mouse monoclonal anti-differentiated cluster Kappa antibodies (dilution, 1:2500; catalog number, AB81289; Abcam, Cambridge, UK) during antigen recovery and endogenous peroxidase treatment. All reactions were performed by automatic immunostaining (DakoCytomation, Carpenteria, CA, USA) and Envision immunostaining-HRP detection system (Dako Cytomation), and diaminobenzidine was used as chromogen. Using the Aperio Scan Scope CS digital imaging system to scan slices and Spectrum (Aperio Technologies, Vista, CA, USA) to process the images.

Statistical Analysis

All values were expressed as mean±s.e. of the mean, unless indicated otherwise. SPSS 21.0 software (IBM, Armonk, NY, USA) was used for statistical analysis. Single factor analysis of variance (ANOVA) was used in the in vivo experiments. $p<0.05$, it was considered the difference was statistically significant.

Results

Effects of PX-12 on Cell Activity and Cell Cycle Distribution in H929 Cells

After exposure to concentration range of 1-30 μM PX-12 for 72h, the viability of H929 cells was not affected at 1 μM PX-12, whereas 2.5 and 5.0 μM PX-12 treatment could induce cell death of H929 cells. In addition, the number of cells was decreased significantly at 5.0-30.0 μM PX-12 (Figure 1A). Based on MTT assays, compared with the DMSO control group, the cell viability

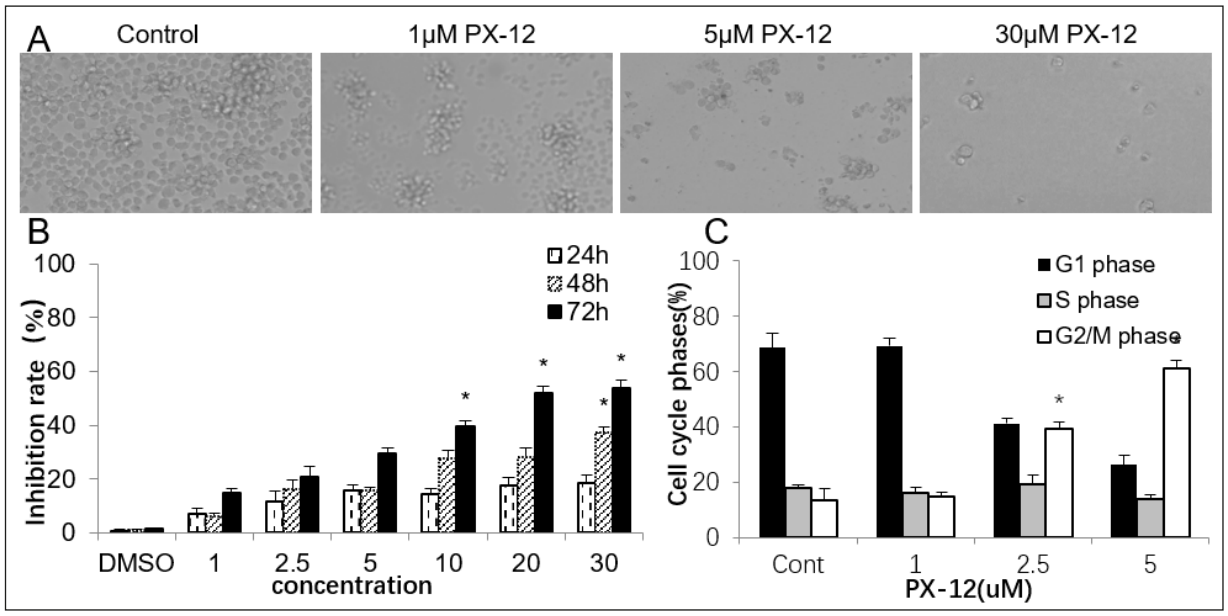

Figure 1. Effects of PX-12 on growth and cycle distribution in H929 cells. **A**, Figures indicate cell population of H929 cells treated by PX-12 at 72h (×200). **B**, Cell viability changes in H929 cells assessed by MTT assays. **C**, Changes in the cell cycle distributions assessed by DNA flow cytometric analysis at 72h. *$p<0.05$, compared with the control group. MTT, 3-(4,5-dimethylthiazol-2-yl)-2,5-diphenyltetrazolium bromide.

dropped sharply at the dose of 5.0 μM tested at 24h, and significantly decreased at 72h, the high dose of 30.0 μM PX-12 inhibited the growth of H929 cells most significantly at 24h; however, there was no difference at 72h (Figure 1B). By examining the cell cycle distribution of H929 cells treated with PX-12, it was found that 2.5 and 5.0 μM PX-12 significantly induced cell cycle arrest in G2 and M phase at 72h (Figure 1C).

Effects of PX-12 on Cell Apoptosis in H929 Cells

As shown in Figure 2B, after 72 hours of treatment, 10 μM PX-12 could increase the percentage of Annexin V FITC positive cells, while 1 μM PX-12 could not increase the percentage of cells (data not shown). We also observed the effects of NAC and BSO on apoptosis of H929 cells treated with 10 μM PX-12. As shown in Figure 2A, NAC significantly reduced the apoptosis of H929 cells treated with PX-12, while BSO increased the number of apoptotic cells. NAC and BSO had no significant effect on the growth and apoptosis of H929 cells (data not shown).

Effects of PX-12 on the Level of ROS and Caspase-3 in H929 Cells

H_2DCFDA probe was performed to evaluate the intracellular ROS level in PX-12 treated H929 cells. As shown in Figure 3A, PX-12 could significantly increase the intracellular ROS (H_2DCFDA) level of H929 cells at the dose of 2.5 μM-10 μM after 72 h. Among the different concentrations, 10 μM PX-12 resulted in the highest level of ROS, while the ROS level decreased at the dose 20 μM and 30 μM (Figure 3A). ROS level was increased sharply in a dose of 10 μM at 72 h, the effects of NAC or BSO on ROS level at 10 μM PX-12 treated H929 cells were detected after 72 h. As shown in Figure 3B, treatment of cells by combination of NAC (2 mM) and PX-12 (10 μM) could significantly rescue H929 cells from undergoing cell death, whereas BSO increased the level again. NAC and BSO had no significant effect on ROS level in the control group (data not shown). The caspase-3 activity was used to detect the apoptosis-inducing effect of PX-12 on H929 cells. Compared with untreated cells, the caspase-3 activity of H929 cells significantly increased by 4 times after being treated with 10 μM PX-12 for 72 h. NAC markedly attenuated the caspase-3 activity increasing in PX-12-treated H929 cells. However, BSO did not affect the caspase-3 level caused by PX-12 (Figure 3C).

PX-12 Decreased the Trx-1 Level of Serum in MM Mice Model Established by H929/EL Cells

Trx-1 is located in the cytoplasm and nucleus and increase in the serum of tumor model ani-

mals and tumor patients. In this study, the level of Trx-1 in the serum of multiple myeloma SCID mice was detected by ELISA kit. To compare the tumor tissue cell activity, the tumor intracellular detection was not detected. In the *in vivo* study, mice were treated with PX-12 (8 mice/group) for 6 weeks, as assessed by measurement of serum Trx-1 level between control group and PX-12 treated group by ELISA Kit. As was shown, serum TRX-1 level in SCID mice were very low, while serum TRX-1 level in myeloma SCID-rab mice was much higher (Figure 4A). After exposed to PX-12 for 2h, serum Trx-1 level in the myeloma SCID-rab mice model caused significantly decrease, there was still a reduction up to 24h after PX-12 treatment, compared with the control group (Figure 4B), but there was no difference between 2h and 24h.

PX-12 Inhibited Tumor Growth in Mice Model Established by H929/EL Cells

To observe the impeded effect of PX-12 on MM *in vivo*, SCID-rab model was established by H929/EL cells, specific methods refer to article published by Yata et al[23]. Mice model were administered PX-12 (dissolved in DMSO), 25 mg/kg intravenously, tumor burden was monitored by the Living-Imaging every 7 days. As shown in Figure 5, tumor grows very rapidly in the control group, especially after 21 days; however, tumor grows extremely slow in the PX-12 group, the maximum diameter of tumor in PX-12 group and control group was 11.5 mm and 24.2 mm, respectively, the median diameters of tumors in PX-12 group and control group were 11.2±0.3 mm and 23.5±0.7 mm, respectively (p<0.01). Tumor cell proliferation in the control group was sharp, it increased by 3-fold in the 21days compared to PX-12 group detected by Living-Imaging (p<0.01).

Histological Analysis of MM Tumor In Vivo Growth Affected by PX-12

As assessed by immunohistochemical staining, morphologically, myeloma cells infiltration in the tumor tissue reduced at the PX-12 treatment group from control hosts when stained for H&E (Figure 6A, B), anti-Kappa staining showed that the number of myeloma cells treated with px-12 was significantly lower than that of the control group (Figure 6C, 6D). It was shown that PX-12 could inhibit the growth of myeloma cells in SCID-rab mice as evaluated by immunohistochemical staining 6 weeks after treatment.

Discussion

The Trx system maintains the redox dynamic balance of cells by directly scavenging ROS or regulating several redox enzymes[24]. Wherein,

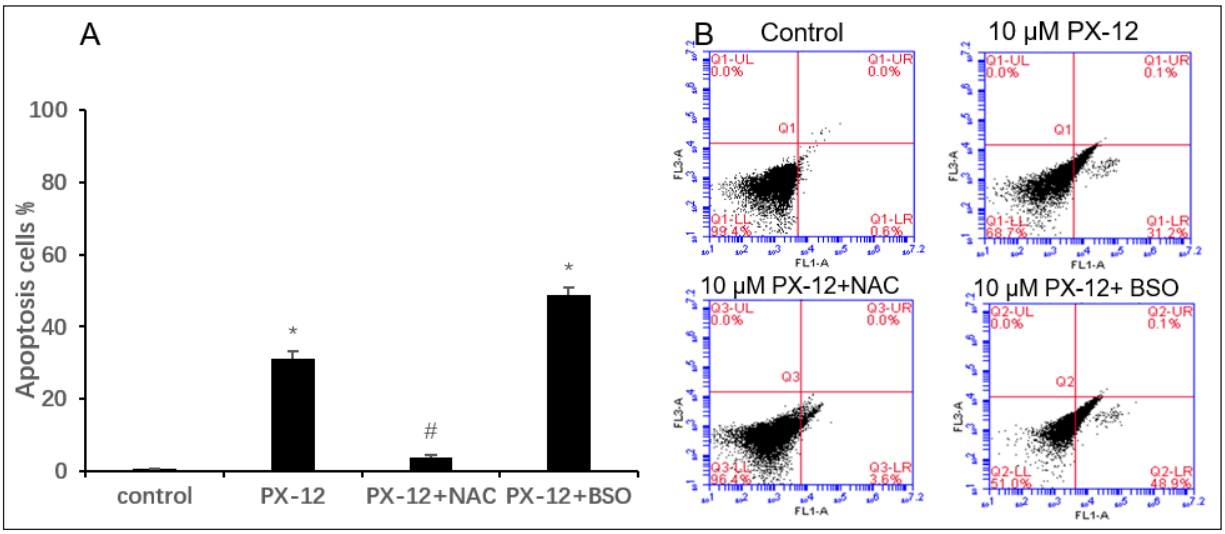

Figure 2. Effects of PX-12 on cell death and affected by the NAC and BSO. Exponentially growing cells were treated with 10 μM PX-12 for 72 h following 1 h pre-incubated with 2 mM NAC or 10 μM BSO. The cell apoptosis was detected by the FACStar flow cytometer. **A**, Indicated the percentage of Annexin V-positive cells. **B**, It shows cell apoptosis of PX-12 treated H929 cells and affected by the NAC and BSO. *p<0.05, compared with the control group; # p>0.05, compared with control group. NAC, N-acetyl cysteine; BSO, L-buthionine sulfoximine; PI, propidium iodide.

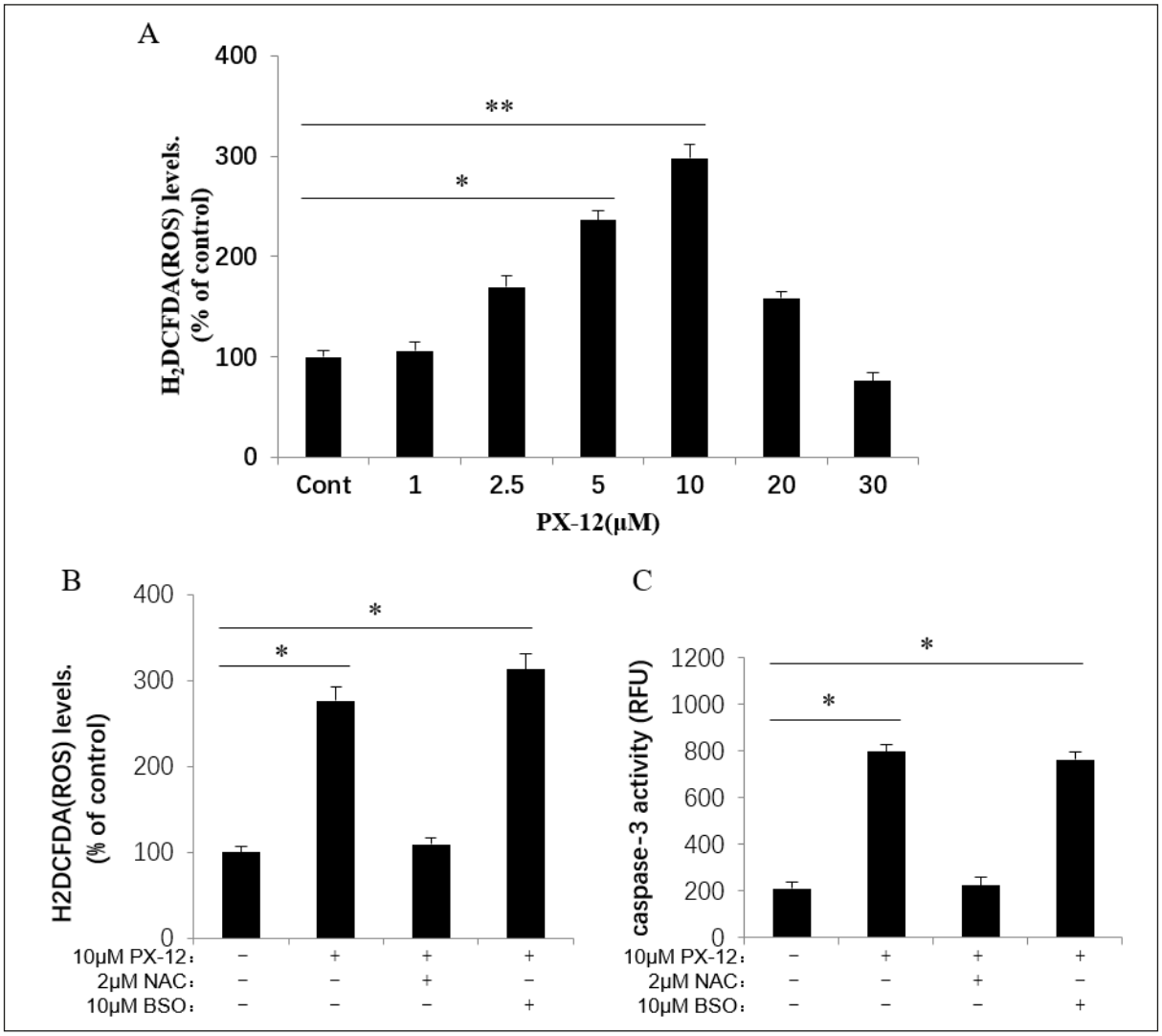

Figure 3. Effects of PX-12 on the intracellular ROS level in H929 cells. Exponentially growing cells were treated with the indicated concentrations of PX-12 for 72 h. ROS level in H929 cells was measured using a FACS flow cytometer. **A**, H2DCFDA (ROS) level as a percentage of the control. The caspase-3 activity was measured to determine the apoptosis induced by PX-12 on H929 cells. **B**, Effects of NAC and BSO on ROS levels in PX-12-treated H929 cells. Exponentially growing cells were treated with 10 μM PX-12 for 72 h following 1 h pre-incubation with 2 mM NAC or 10 μM BSO. Graph showed ROS levels as a percentage of the control, the increased ROS levels were prevented by NAC but not BSO. **C**, Caspase-3 activity increased by 4-fold treated with 10 μM PX-12 at 72h compared to non-treated cells, NAC markedly attenuated the caspase-3 activity increasing by PX-12 and BSO did not affect the caspase-3 level caused by PX-12, *$p<0.05$, compared with the control group.

Trx-1 plays a critical role in cell survival, angiogenesis, tumor proliferation and metastasis[25]. It is overexpressed in kinds of human cancers including cervical, lung, gastric, colon, breast and pancreatic cancer, which can increase production of VEGF and promote tumor angiogenesis[26-30]. Nakamura et al[31] have reported that plasma TRX-1 levels were increased in patients with pancreatic cancer and hepatocellular carcinoma. A couple of studies[19,20,22] have shown that thioredoxin expression is increased in the patients with T-ALL, lymphoma and myeloma. Therefore, Trx-1 inhibitors have been considered as new type of antineoplastic drugs, particularly, PX-12 is an irreversible Trx-1 inhibitor, which has an anti-tumor effect in a variety of human tumors including acute myeloid leukemia, lymphoma, myeloma[21], colorectal cancer[16], cervical cancer[32] and lung cancer[17].

In our study, it was showed that PX-12 inhibited proliferation of H929 cells after 72h treatment at dose from 5.0 to 30.0 μM (Figure 1A, B), growth inhibition of H929 cells performed time-

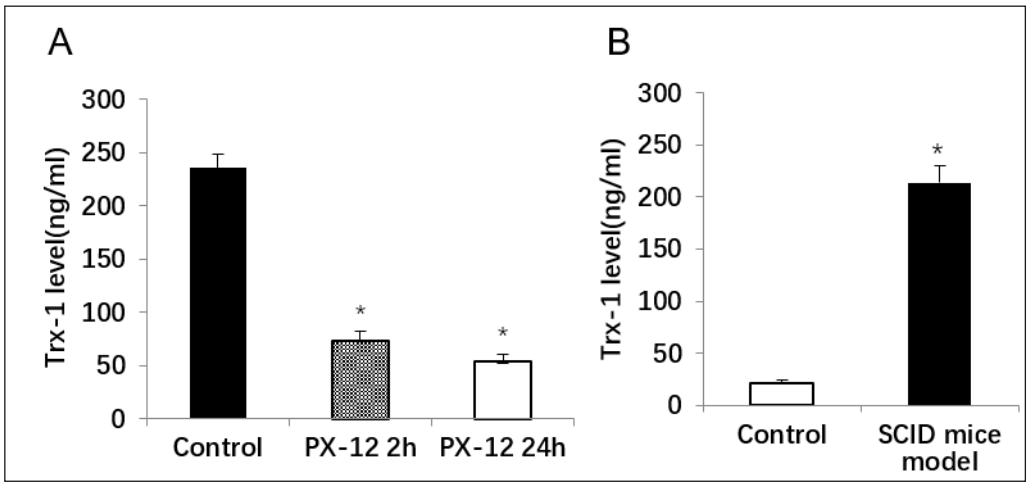

Figure 4. Serum Trx-1 level was assessed by ELISA Kit. **A**, Serum Trx-1 level in the mice without tumor was low, and sharply increased in the myeloma SCID-rab mice model. **B**, Serum Trx-1 level in the myeloma SCID-rab mice model significantly reduced after 2h and 24h treated with indicated concentrations of PX-12 compared with the control group. *p<0.05, compared with the control group.

and dose-dependent style. Furthermore, it significantly induced cell cycle arrest of H929 cells in G2/M phase (Figure 1C). Similarly, it has been found that PX-12 induces a G2/M phase arrest in other cancer cells such as lung cancer, breast cancer and B-cell lymphoma.

The effects of PX-12 on the growth and apoptosis of H929 cells in relation to ROS and caspase-3 level were also investigated in the experiment, as was shown, PX-12 increased intracellular ROS and caspase-3 activity in H929 cells, suggesting that apoptosis occurred in H929 cells (Figures 2 and 3).

To our knowledge, elevated TRX-1 levels are related to tumor chemotherapy resistance, and inhibition of Trx1 could reverse the drug resistance of many tumors.

PX-12, an irreversible inhibitor of Trx1, has been shown to inhibit tumor growth and lead to ROS-induced apoptosis in many human cancers including AML, MM. However, *in vivo* studies on anti-myeloma activity of PX-12 were rarely reported. It was showed that MM cells have increased Trx-1 expression levels compared to the normal PBMCs22. We used H929 cells to verify the inhibitory effect of PX-12 on different multiple myeloma cells, and constructed the multiple myeloma SCID mice model and further analyzed the *in vivo* inhibitory effect of PX-12 on multiple myeloma cells. In the present studies, for the first time, we analyzed expression of Trx-1 in serum from SCID-rab mice model, it was (±S.E) 213.68±16.97 ng/ml, which increased dramatically when compared to the hosts without tumor (±S.E)21.02±3.27 ng/ml (p<0.05) (Figure 4A), this was similar as reported.

Two hours after intravenous injection of PX-12 25 mg/kg, a significant decrease in plasma Trx-1 was observed (±S.E) 73.19±8.67 ng/ml and remained inhibited by (±S.E) 53.47±7.37 ng/ml at 24 hr, much lower compared with the control group of (±S.E) 235.67±13.52 ng/ml (p<0.05) (Figure 4B). We observed that PX-12 decreased levels of circulating Trx-1 in myeloma bearing mice model.

This study showed that PX-12 inhibited MM cells growth in the SCID-rab mice model. As mentioned, H929EL cells' viability was also decreased by PX-12 treatment *in vivo*, there was no significant inhibition in xenografts growth observed in control group (Figure 5 A, B). We observed that cells proliferation also significantly decreased in PX-12 treated xenografts 14 days after drug injection compared with untreated controls. There was almost 3-5-fold decrease in tumor viability measured by Living-Imaging system after 21 and 28 days later injected PX-12 compared with the control group. Importantly, PX-12 caused significant decreases in expression of Kappa chain *in vivo* assessed by immunohistochemical staining (Figure 6 C, D).

Conclusions

In summary, PX-12 could inhibit the proliferation of H929EL cells via G2/M phase arrest, and ROS-dependent apoptosis. Furthermore, we

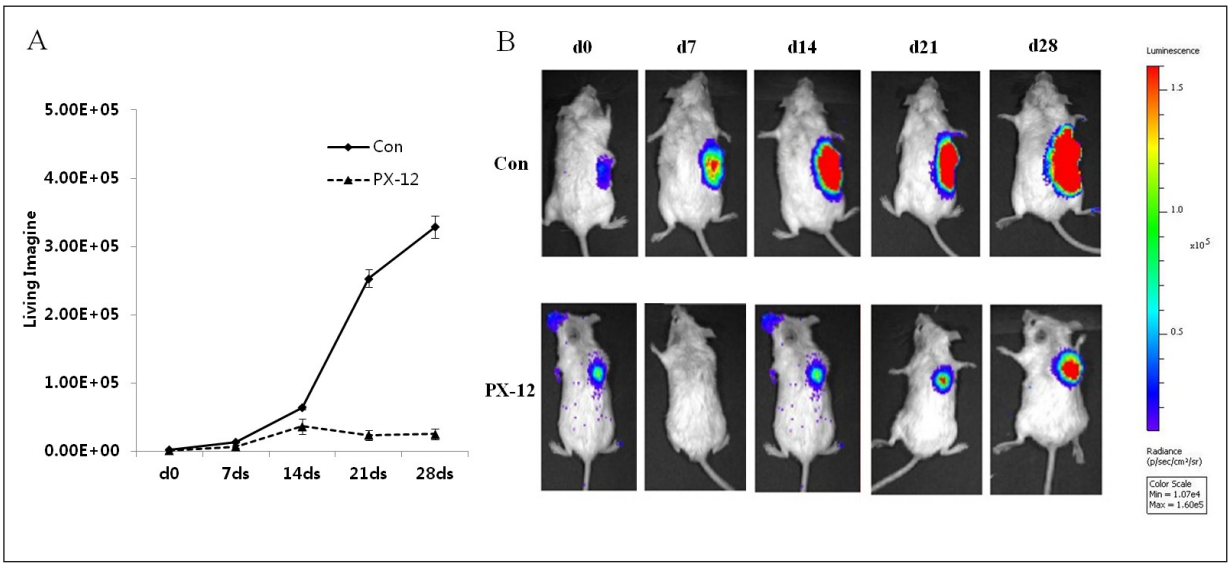

Figure 5. Living-Imaging system assessed the effect of PX-12 on the SCID-RAB mice model established by H929/EL cells. Mice model were treated with PX-12(dissolved in DMSO), 25 mg/kg intravenously. **A**, The growth of Luciferase expressing in control group (mice treated with DMSO) was shown measured by the Living-Imaging system, Luciferase expressing in SCID-RAB mice model in the PX-12 treated model were much lower than control group when detected at 21 days and 28 days (p<0.01). **B**, Changes in bioluminescence intensity of the implanted bones engrafted H929/EL cells to the SCID-RAB mice, tumor burden of mice in the control group were much higher than in the PX-12 treated model, especially detected at 21 days and 28 days.

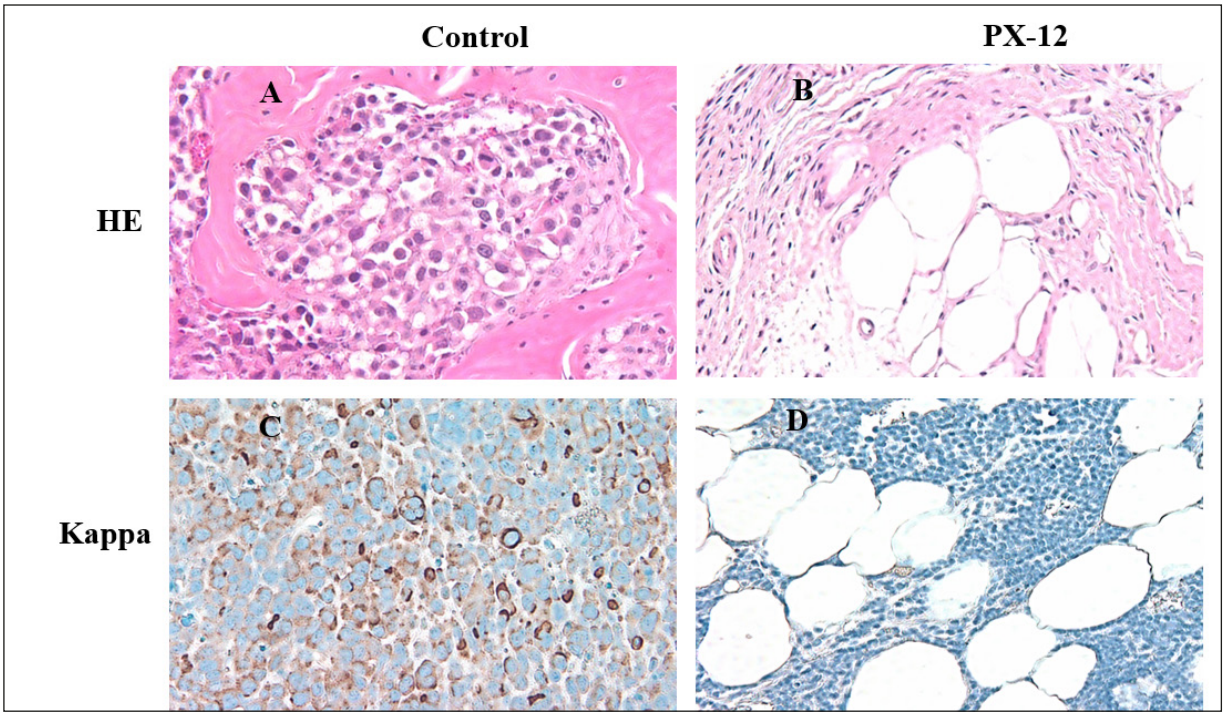

Figure 6. Micrographs showed hematoxylin and eosin staining of tumor tissue from control and PX-12 treated mice model (**A, B**), less MM cell infiltration in the tumor of PX-12 treated mice (**B**) than of the control group (**A**). Kappa staining of tumor tissue performed more positive cells in the control group (**C**) than in the PX-12 treated mice (**D**) (×200).

first reported that Trx-1 level increased in the H929EL/SCID-rab mice model, and PX-12 could decrease Trx-1 level *in vivo*, as well as inhibited MM cells growth in the SCID-rab mice model. This research provided both *in vitro* and *in vivo* evidence about anti myeloma effect of PX-12 which may provide ideas for the development of new and more effective methods for the treatment of MM.

Acknowledgment
The authors would like to thank the patients, researchers, and staff involved in this study.

Funding
This study was supported by the Zhengzhou Science and Technology Project grant (No. 153PKJGG060) funded by the Zhengzhou Technology Bureau and Henan Province medical science and technology research project (201602287) supported by the Health and Family Planning Commission of Henan Province.

Authors' Contributions
QD Lin, and YP Song designed the outline of the study, LN Liu, XY Liu, Y Yan, BJ Fang, designed the study, conducted experiments and wrote the manuscript, YL Zhang, J Zhou, YF Li and WL Zuo, supervised the study, contributed to data acquisition and revised the manuscript. QD Lin, YF L, and YP Song, collected and analyzed the data. All authors have read and approved the final version of this manuscript.

Ethics Approval and Consent to Participate
The animal experiment was approved by the Ethics Committee of Henan Cancer Hospital.

Patient Consent for Publication
Not applicable.

Conflicts of Interest
The authors declare no conflicts of interest.

References

1) Raab MS, Podar K, Breitkreutz I, Richardson PG, Anderson KC. Multiple myeloma. Lancet 2009; 374: 324-339.
2) Agarwal A, Mahadevan D. Novel targeted therapies and combinations for the treatment of multiple myeloma. Cardiovasc Hematol Disord Drug Targets 2013; 13:2-15.
3) Avet-Loiseau H, Bahlis NJ, Chng WJ, Masszi T, Viterbo L, Pour L, Ganly P, Palumbo A, Cavo M, Langer C, Pluta A, Nagler A, Kumar S, Ben-Yehuda D, Rajkumar SV, San-Miguel J, Berg D, Lin J, van de Velde H, Esseltine DL, di Bacco A, Moreau P, Richardson PG. Ixazomib significantly prolongs progression-free survival in high-risk relapsed/refractory myeloma patients. Blood 2017; 130: 2610-2618.
4) Yucai Wang, Larysa Sanchez, David S. Siegel, Michael L Wang. Elotuzumab for the treatment of multiple myeloma. J Hematol Oncol 2016; 9: 55.
5) Mateos MV, Dimopoulos MA, Cavo M, Suzuki K, Jakubowiak A, Knop S, Doyen C, Lucio P, Nagy Z, Kaplan P, Pour L, Cook M, Grosicki S, Crepaldi A, Liberati, AM, Campbell P, Shelekhova T, Yoon SS, Iosava G, Fujisaki T, Garg M, Chiu C, Wang JP, Carson R, Crist W, Deraedt W, Nguyen H, Qi M, Miguel JS. Daratumumab plus Bortezomib, Melphalan, and Prednisone for Untreated Myeloma. N Engl J Med 2018; 378: 518-528.
6) Ali SA, Shi V, Maric I, Wang M, Stroncek DF, Rose JJ, Brudno JN, Stetler-Stevenson M, Feldman SA, Hansen BG, Fellowes VS, Hakim FT, Gress RE, Kochenderfer JN. T cells expressing an anti-B-cell-maturation-antigen chimeric antigen receptor cause remission of multiple myeloma. Blood 2016; 128: 1688-1700.
7) Jemal A, Bray F, Center MM, Ferlay J, Ward E, Forman D. Global cancer statistics. CA Cancer J Clin 2011; 61: 69-90.
8) Lu J, Holmgren A.The thioredoxin antioxidant system. Free Radic Biol Med 2014; 66:75-87.
9) Lincoln DT, Emadi EMA, Tonissen KF, Clarke FM. The thioredoxin-thioredoxin reductase system: over-expression in human cancer. Anticancer Res 2003; 23: 2425-2433.
10) Kim SJ, Miyoshi Y, Taguchi T, Tamaki Y, Nakamura H, Yodoi J, Kato K, Noguchi S.High thioredoxin expression is associated with resistance to docetaxel in primary breast cancer. Clin Cancer Res 2005; 11: 8425-8430.
11) Li CP, Thompson MA, Tamayo AT, Zuo Z, Lee J, Vega F, Ford RJ, Pham LV. Over-expression of Thioredoxin-1 mediates growth, survival, and chemoresistance and is a druggable target in diffuse large B-cell lymphoma. Oncotarget 2012; 3: 314-326.
12) Pramanik KC, Srivastava SK. Apoptosis signal-regulating kinase 1-thioredoxin complex dissociation by capsaicin causes pancreatic tumor growth suppression by inducing apoptosis. Antioxid Redox Signal 2012; 17: 1417-1432.
13) Dunn LL, Buckle AM, Cooke JP, Ng MK. The emerging role of the thioredoxin system in angiogenesis. Arterioscler Thromb Vasc Biol 2010; 30: 2089-2098.
14) Liu JJ, Liu Q, Wei HJ, Yi J, Zhao HS, Gao LP. Inhibition of thioredoxin reductase by auranofin

induces apoptosis in adriamycin-resistant human K562 chronic myeloid leukemia cells. Pharmazie 2011; 66: 440-444.

15) Pan D, Li W, Miao HC, Yao J, Li ZY, Wei LB, Zhao L, Guo QL. LW-214, a newly synthesized flavonoid, induces intrinsic apoptosis pathway by down-regulatingTrx-1in MCF-7 human breast cells. Biochem Pharmacol 2014; 87: 598-610.

16) Wang FL, Lin FY, Zhang PL, Ni WH, Bi LX, Wu JB, Jiang L. Thioredoxin-1 inhibitor, 1-methylpropyl 2-imidazolyl disulfide, inhibits the growth, migration and invasion of colorectal cancer cell lines. Oncol Rep 2015; 33:967-973.

17) You BR, Shin HR, Park WH. PX-12 inhibits the growth of A549 lung cancer cells via G2/M phase arrest and ROSdependent apoptosis. Int J Oncol 2014; 44: 301-308.

18) Baker AF, Dragovich T, Tate WR, Ramanathan RK, Roe D, Hsu CH, Kirkpatrick DL, Powis G. The antitumor thioredoxin-1 inhibitor PX-12 (1-methylpropyl 2-imidazolyl disulfide) decreases thioredoxin-1 and VEGF levels in cancer patient plasma. J Lab Clin Med 2006; 147: 83-90.

19) Shao L, Diccianni MB, Tanaka T, Gribi R, Yu AL, Pullen JD, Camitta BM, Yu J. Thioredoxin expression in primary T-cell acute lymphoblastic leukemia and its therapeutic implication. Cancer Res 2001; 61: 7333-7338.

20) Kari EJM, Kuusisto MEL, Honkavaara P, Hakalahti A, Haapasaari KM, Bloigu R, Karihtala P, Teppo HR, Pirinen R, Hujanen TT, Kuittinen O. Thioredoxin-1 as a biological predictive marker for selecting diffuse large B-cell lymphoma patients for etoposide-containing treatment. Eur J Haematol 2020; 105: 156-163.

21) Tan Y, Bi LX, Zhang PL, Wang FL , Lin FY, Ni WH, Wu JB, Jiang L. Thioredoxin-1 inhibitor PX-12 induces human acute myeloid leukemia cell apoptosis and enhances the sensitivity of cells to arsenic trioxide. Int J Clin Exp Pathol 2014; 7: 4765-4773.

22) Raninga PV, Trapani GD, Vuckovic S, Bhatia M, Tonissen KF. Inhibition of thioredoxin 1 leads to apoptosis in drug-resistant multiple myeloma. Oncotarget 2015; 6:15410-15424.

23) Yata K, Yaccoby S. The SCID-rab model: a novel in vivo system for primary human myeloma demonstrating growth of CD138-expressing malignant cells. Leukemia 2004; 18: 1891-1897.

24) Kim HY, Kim JR. Thioredoxin as a reducing agent for mammalian methionine sulfoxide reductases B lacking resolving cysteine. Biochem Biophys Res Commun 2008; 371: 490-494.

25) Welsh SJ, Bellamy WT, Briehl MM, Powis G. The redox protein thioredoxin-1 (Trx-1) increases hypoxia-inducible factor 1alpha protein expression: Trx-1 overexpression results in increased vascular endothelial growth factor production and enhanced tumor angiogenesis. Cancer Res 2002; 62: 5089-5095.

26) Powis G, Montfort WR. Properties and biological activities of thioredoxins. Annu Rev Pharmacol Tox 2001; 41: 261-295.

27) Lim JY, Yoon SO, Hong SW, Kim JW, Choi SH, Cho JY. Thioredoxin and thioredoxin-interacting protein as prognostic markers for gastric cancer recurrence. World J Gastroenterol 2012; 18: 5581-5588.

28) Cha MK, Suh KH, Kim IH. Overexpression of peroxiredoxin I and thioredoxin 1 in human breast carcinoma. J Exp Clin Cancer Res 2009; 28: 93.

29) Fath MA, Ahmad IM, Smith CJ, Spence JL, Spitz DR. Enhancement of carboplatin mediated lung cancer cell killing by simultaneous disruption of glutathione and thioredoxin metabolism. Clin Cancer Res 2011; 17: 6206-6217.

30) Fernandes AP, Capitanio A, Selenius M, Brodin O, Rudolf AK, Björnstedt M. Expression profiles of thioredoxin family proteins in human lung cancer tissue: correlation with prolifera¬tion and differentiation. Histopathology 2009; 55: 313-320.

31) Nakamura H, Bai J, Nishinaka Y, Ueda S, Sasada T, Ohshio G, Imamura M, Takabayashi A, Yamaoka Y, Yodoi J. Expression of thioredoxin and glutaredoxin, redox-regulating proteins, in pancreatic cancer. Cancer Detect Prev 2000; 24: 53-60.

32) Hye RS, You BA, Park WH. PX-12 induced HeLa cell death is associated with oxidative stress and GSH depletion. Oncol Lett 2013; 6: 1804-1810.